Density-functional study of structural and electronic properties of Na_nLi and Li_nNa $(1 \leqslant n \leqslant 12)$ clusters

M. D. Deshpande* and D. G. Kanhere*
Department of Physics, University of Pune, Pune 411007, India

Igor Vasiliev† and Richard M. Martin†
Department of Physics, University of Illinois at Urbana-Champaign, Urbana, Illinois 61801
(Received 23 August 2001; published 8 February 2002)

Equilibrium geometries and electronic-structure properties of Na_nLi and Li_nNa $(n=1-12)$ clusters are obtained using *ab initio* molecular-dynamics method with the generalized gradient approximation for the exchange-correlation potential. The resulting geometries show that Li atoms become trapped inside the Na cage, while Na prefers to be on the periphery of Li clusters. The comparison of total binding energies indicates a high degree of stability for clusters with eight atoms. We also report polarizabilities for both series of Na_nLi and Li_nNa clusters. Polarizabilities are calculated by a finite field method. Our calculations demonstrate that Li impurity reduces polarizabilities of Na_n clusters while the doping of Na in Li_n clusters increases the polarizabilities.

DOI: 10.1103/PhysRevA.65.033202 PACS number(s): 36.40.Qv, 36.40.Mr, 61.46.+w, 31.15.Ar

I. INTRODUCTION

The physics and chemistry of alkali-metal clusters has been the subject of intensive research, especially during the last decade. Perhaps the most well-studied systems are the clusters of simple metals such as Na, Li, Al, and Mg. Most of the reported work has been carried out on homogeneous clusters [1–8]. Different quantum computational models, including density-functional formalism, have been employed to probe their electronic structure, the later ones usually in conjunction with molecular dynamics. One of the interesting questions pertains to the properties of impurity-induced defects. The structures and electronic properties of clusters doped with a single impurity have been the subject of several recent theoretical studies. These studies include density-functional calculations on the equilibrium geometries, energetics, and stability of Li_nBe [9], Li_nMg [9], Li_nAl [10], Na_nLi [11], Na_nMg [12–14], Na_nAl [15], Al_nLi [16], and Al_nNa [17,18]. The calculations reveal that impurities with smaller ionic radii and a strong binding with the host become trapped in the cluster. Impurities often lead to an early appearance of three-dimensional (3D) geometries as compared to the host clusters. It has also been observed that divalent impurities, such as Be and Mg could induce different geometries and growth paths in a monovalent Li host [9].

In the present work, we carry out a systematic investigation of Na_nLi and Li_nNa $(n=1-12)$ clusters. In both cases, a monovalent impurity is doped in a monovalent host. Our calculations are performed by standard *ab initio* molecular dynamics within the framework of density-functional theory (DFT) using the simulated annealing strategy.

In addition, we calculate the static polarizability for both series of Na_nLi and Li_nNa clusters. The static polarizability is one of the essential electronic properties of clusters that can be directly measured in experiments. It is known to be sensitive to the charge density distribution and the degree of delocalization of the valence electrons. Despite a large number of works devoted to alkali-metal clusters, the experimental measurements of polarizabilities are available only for Li, Na, and K clusters [19–24]. The experimental polarizabilities for the dimer, trimer, and tetramers of NaLi clusters have been reported by Antoine *et al.* [25]. We focus on the evolution of static polarizabilities for both series of Na_nLi and Li_nNa clusters as a function of cluster size and compare the results with the available experimental data.

II. COMPUTATIONAL DETAILS

All our simulations were carried out using *ab initio* Born-Oppenheimer molecular-dynamics. Towards this end, we have used an efficient scheme based on damped second-order equation of motion and the integration scheme proposed by Payne *et al.* [26] This has permitted us to use a fairly moderate time step $\approx$100 a.u. Cluster geometries were obtained by starting with unbiased configuration which then was heated up to 600–800 K and slowly cooled down to zero temperature. We used norm conserving nonlocal pseudopotential of Bachelet, Hamann, and Schluter [27] with the *p* component taken as local and the von Barth-Hedin approximation for the exchange-correlation potential [28]. All calculations were carried out within a periodic cell with a side of 40 a.u. The energy cutoff in our calculations was set at 11 rydberg. In all cases, the stability of the ground-state configuration was tested by reheating the cluster and allowing it to span in the configuration space, and then cooling it to get the lowest-energy configuration. The final structures were obtained by the steepest-descent method starting from suitable configuration during the simulated annealing run. Many of the low-energy structures were verified by interchanging the positions of Li and Na atoms and repeating the annealing procedure. The structures obtained from the above procedure

*Email address: mdd,kanhere@physics.unipune.ernet.in
†Email address: vasiliev,rmartin@uiuc.edu

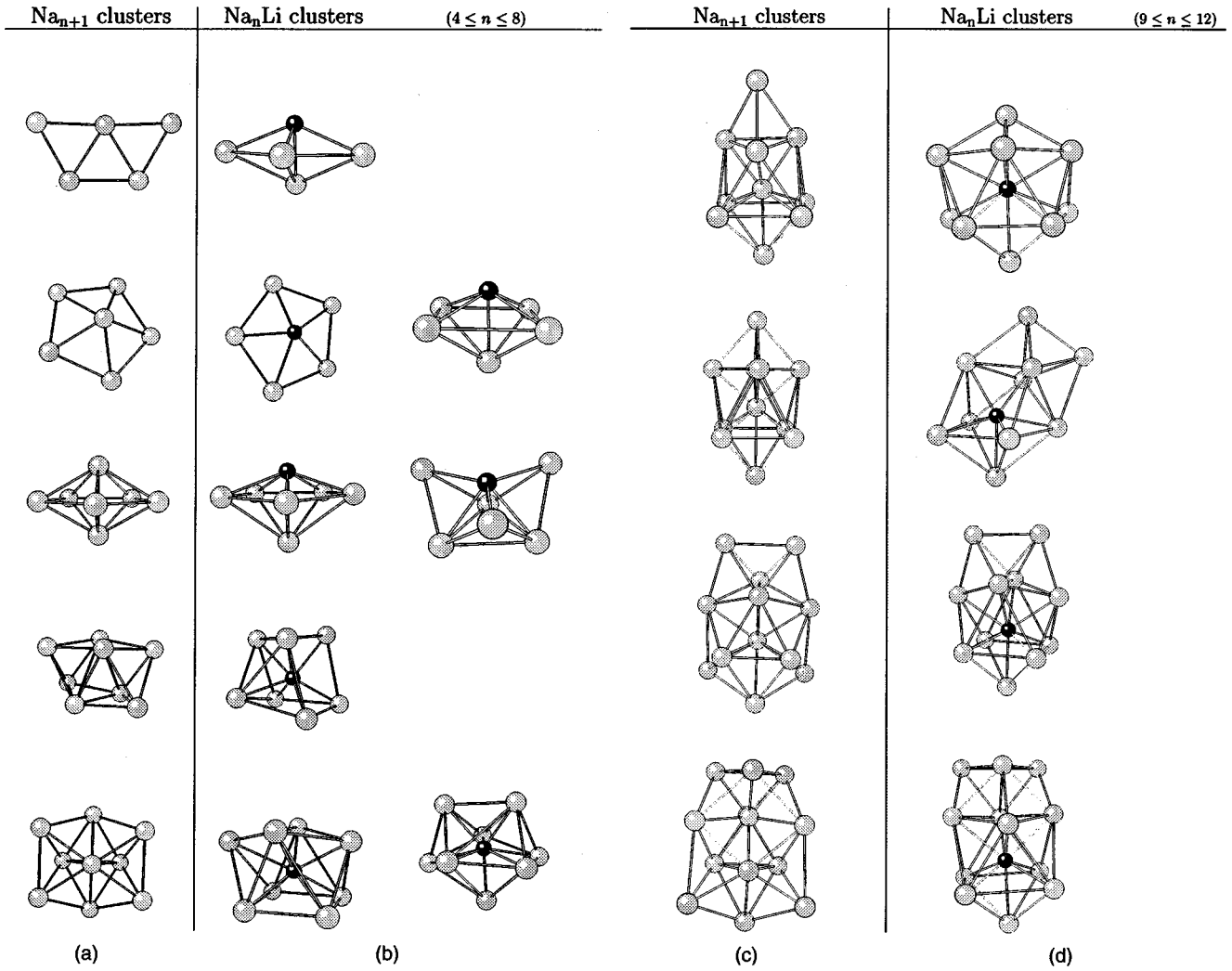

FIG. 1. Ground-state geometries of Na_{n+1} clusters (column 1). The structures on the right side show the lowest-energy structures (columns 2) and some of the low-energy isomers (columns 3) for Na_nLi clusters. Lithium atoms are represented by the dark circles.

were further refined by using a real-space technique [29]. The real-space calculations were performed using a higher-order finite difference method [30]. In our calculations, we used a grid spacing of $h=0.4$ a.u. The grid was set up inside a spherical boundary with a radius of 15 a.u. The exchange-correlation potential in these calculations was computed with the generalized gradient approximation (GGA) of Perdew *et al.* [31].

Polarizabilities were calculated using a finite-field approach [23,29]. To do so, the Kohn-Sham equations were solved with and without a small electric field applied to the cluster of interest. The polarizability is defined by

$$\alpha_{ij}=\frac{\partial \mu_i(F)}{\partial F_j}=-\frac{\partial^2 E(F)}{\partial F_i \partial F_j}, \tag{1}$$

where $i,j=\{x,y,z\}$ and the dipole moment is given by

$$\boldsymbol{\mu}(F)=\int \rho(\mathbf{r})\mathbf{r}\,d\mathbf{r}. \tag{2}$$

In Eq. (1), $E(F)$ is the total energy and F_i is the electric field applied along the ith axis. The average polarizability is calculated as the trace of the polarizability tensor, α_{ij},

$$\langle \alpha \rangle=\frac{\alpha_{xx}+\alpha_{yy}+\alpha_{zz}}{3}. \tag{3}$$

The diagonal elements of the polarizability tensor can be obtained either from the dipole moment $\mu(F)$ or from the total energy $E(F)$ calculated at $F=0$ and $F=+\delta F_i$ using the standard finite difference expressions for the first and second derivatives. Polarizability is known to be sensitive to the outer part of the electron density of a cluster. To ensure the proper convergence of the calculated polarizabilities, we increased the radius of the boundary sphere up to 22 a.u. and used a grid spacing of $h=0.6$ a.u. The value of the applied electric field δF was chosen to be 10^{-3} a.u. In all cases, polarizabilities calculated from the total energy and from the dipole moment coincided within 1%.

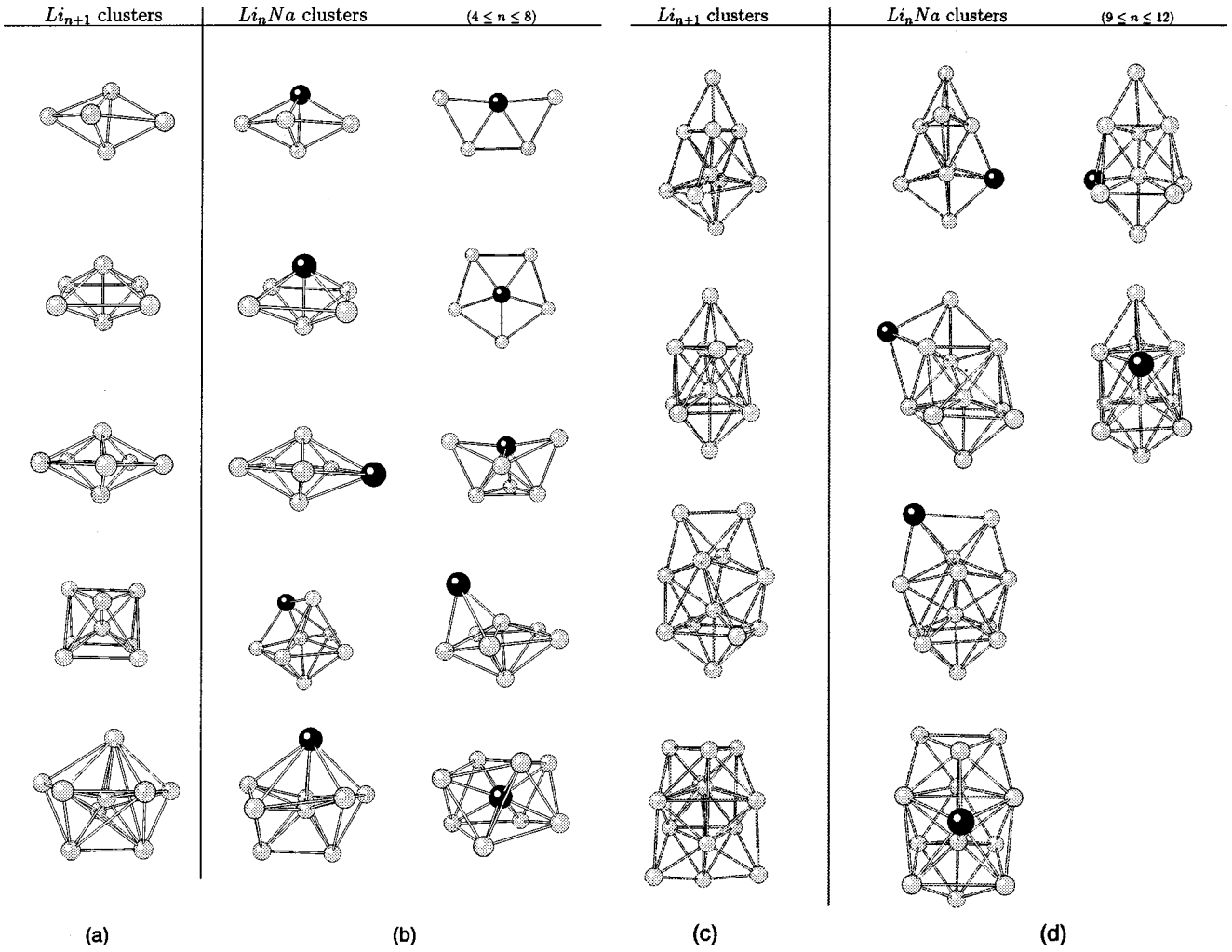

FIG. 2. Ground-state geometries of Li_{n+1} clusters (column 1). The structures on the right side show the lowest-energy structures (columns 2) and some of the low-energy isomers (column 3) for $Li_{n-1}Na$ clusters. Sodium atoms are represented by the dark circles.

III. RESULTS AND DISCUSSION

The equilibrium structures of Na_nLi and Li_nNa ($n=1-12$) along with the geometries of the original host Na_{n+1} and Li_{n+1} clusters are shown in Figs. 1(a), 1(b) and Figs. 2(a), 2(b). In both cases, the impurity atoms are shown as black spheres. We did not include the geometries of clusters with $n \leqslant 3$ in Figs. 1 and 2 because they are very similar to the geometries of Na_{n+1} [1] and Li_{n+1} [2]. Our calculations indicate that doping the planar Na_5 host with Li changes it into a three-dimensional Na_4Li structure. The addition of a single Na atom to Na_4Li generates a pentagonal Na ring with the Li atom taking position slightly above the plane of this pentagon and making this structure to be similar to that of Na_6. Another possible low-energy structure of the Na_5Li cluster is an octahedron with the Li atom at one of the vertices. The pentagonal ring remains intact after the addition of a Na atom to Na_5Li, leading to a pentagonal bipyramid structure where the Li impurity substitutes a Na atom at the apex position. The ground-state structure of the Na_8 cluster is an archimedian antiprism. The substitution of a Na atom with Li distorts the original structure of Na_8 significantly and the impurity becomes trapped almost near the center of the cluster. A similar trapping of the Li atom near the center also occurs in all larger clusters. This trapping is accompanied by considerable distortion of the host structure. The effect of distortion diminishes towards the end of the series.

As in the case of Na_nLi clusters, Li_nNa structures show an early appearance of 3D geometries starting at $n=4$ (Li_4Na). The lowest-energy structure for Li_5Na is the octahedron with the Na atom at one of the vertices. This structure is also similar to that of the Li_6 cluster. Another possible low-energy structure has a planar geometry in which Li atoms form a pentagonal ring with the Na atom at the center. It is interesting to compare geometries of Li_6Na and Na_6Li. Both structures are pentagonal bipyramid, but in the case of Na_6Li, the minimum of the total energy is reached when the Na atom is substituted from the apex position, which maximizes the number of Na-Li bonds. In the case of Li_6Na, the impurity Na atom becomes a part of the pentagonal ring. Structures of all larger clusters are similar to those for pure Li_n with one of the surface Li atoms replaced by Na. It

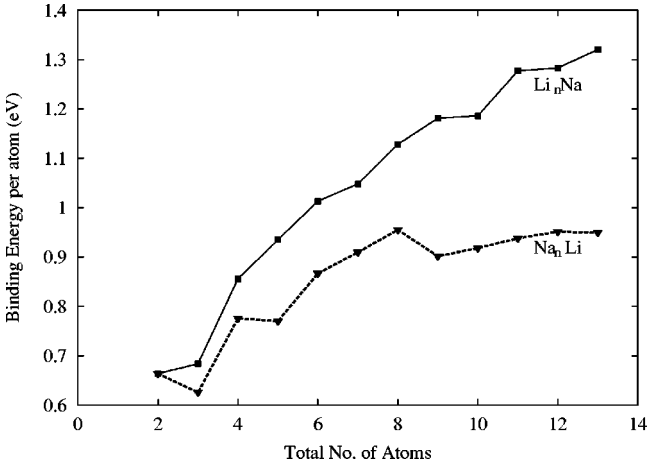

FIG. 3. Binding energy per atom for Li_nNa (solid line) and Na_nLi (dotted line) clusters with ($n=1-12$) vs the total number of atoms.

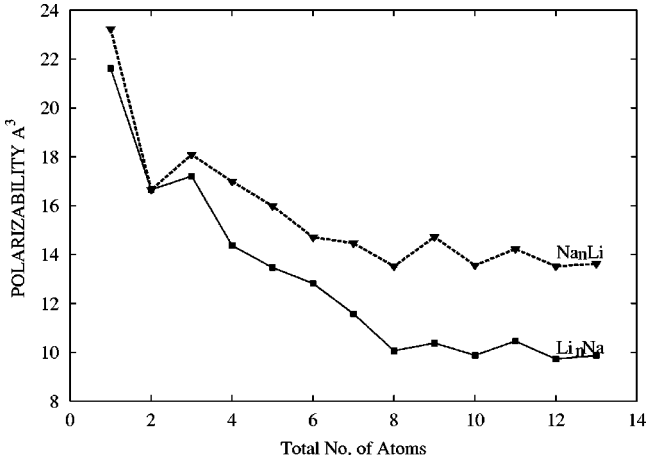

FIG. 4. Polarizabilities of Li_nNa (solid line) and Na_nLi (dotted line) clusters with ($n=1-12$) shown vs the total number of atoms.

should be noted that the energy of the Li-Li bond (0.79 eV) is slightly stronger than that of the Na-Li bond (0.76 eV), which in its turn is slightly stronger than the energy of the Na-Na bond (0.71 eV). The tendency of Na to remain on the surface could, therefore, be attributed to the weaker binding energy as well as to the larger ionic radius of Na (1.80 a.u.) as compared to that of Li (1.13 a.u.).

It is convenient to discuss the stability of Na_nLi and Li_nNa in terms of their binding energies per atom. Figure 3 shows the binding energies per atom for Na_nLi and Li_nNa plotted against the total number of atoms in cluster.

The binding energy per atom is defined as

$$E_b[\mathrm{Na}_n\mathrm{Li}]=(-E[\mathrm{Na}_n\mathrm{Li}]+nE[\mathrm{Na}]+E[\mathrm{Li}])/(n-1), \tag{4}$$

As expected, the binding energies of Li_nNa are higher than that for Na_nLi. Our plot indicates a high stability for clusters with eight-atoms. These features are common for both Na_nLi and Li_nNa clusters and have been observed in other alkali clusters [9,13,15].

We did not observe any significant differences between the local-density approximation (LDA) and GGA optimized geometries for any cluster except for Li_2Na, where the order of the isomer is reversed (in this case, LDA predicts a linear structure, while GGA gives a scalene triangle as the equilibrium geometry). While the switch from LDA to GGA does not seem to affect the overall shapes, GGA calculations predict larger bond lengths than LDA bond lengths. For the diatomic molecule Na-Li, LDA calculations predict the bond length of 5.21 a.u., compared to the GGA bond length of 5.45 a.u. The latter value is much closer to the experimental bond length of 5.54 a.u. This result agrees with a common observation that GGA corrects the overbinding tendency of LDA [13].

Figure 4 shows the average static polarizability (per atom) for Na_nLi, Li_nNa clusters. It should be noted that the atomic polarizabilities are nearly the same for Li (23.6 $Å^3$) and Na (24.6 $Å^3$). In all cases, the polarizabilities of the lithium-rich clusters are lower than that of the sodium-rich clusters (~27%). This trend agrees with other reported calculations [23,22] and experiments [20,22] which indicate that polarizabilities for Na_n are significantly higher than that for Li_n. For example, experimental measurements [22] find the polarizability 16.8 $Å^3$ for the Na_8 cluster as compared to 10.4 $Å^3$ for Li_8. This difference could be explained on the basis of a stronger bonding between Li-Li as compared to Li-Na and Na-Na bond in the cluster. The calculated polarizabilities for both Na_nLi and Li_nNa clusters sharply decrease with increasing the total number of atoms up to $n=8$. After that, the decline slows down considerably and shows the oscillatory behavior with the noticeable dips at $n=10$, 12, which reflect upon the stable nature of the systems.

It is interesting to compare the polarizabilities of these clusters with that of host clusters having the same number of atoms. Figure 5 shows the evolution of polarizabilities for Na_{n+1} [23] along with calculated polarizabilities for Na_nLi. It is observed that doping by Li reduces polarizabilities of Na_n clusters by approximately 5–18 %. The polarizabilities of pure Na clusters show strong oscillations between $n=2-6$. These oscillations are smoothen down upon doping

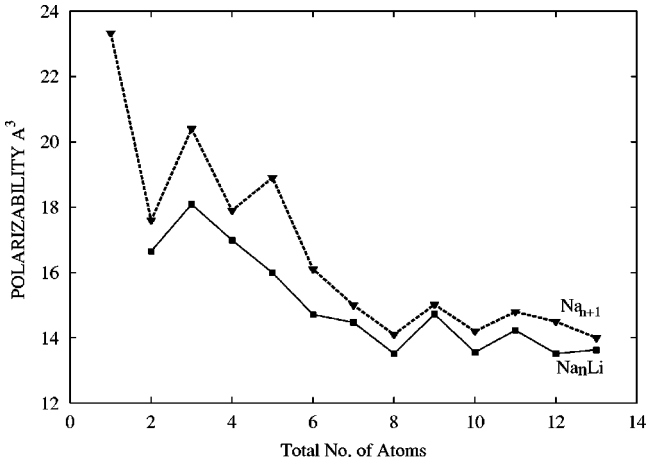

FIG. 5. Polarizabilities of Na_nLi (solid line) and Na_{n+1} [23] (dotted line) clusters with ($n=1-12$) shown vs the total number of atoms.

TABLE I. Average static polarizabilities per atom of dimers, timers, and tetramers of mixed Li-Na clusters in ($Å^3$). By finite field calculation, by DFT/PW91 method, and experimental results.

System	By finite-field method ($Å^3$)	DFT/PW91 ($Å^3$)	Expt. Results ($Å^3$)
Li-Na	16.65	17.7	19.5
Li_2Na	17.21	17.7	11.8
Li_3Na	14.37	15.4	13.7
Na_2Li	18.09	19.5	20.4
Na_3Li	16.99	17.8	18.9

by Li atom. This smoothening is due to significant reduction of polarizability (~18%) at $n=5$ which is caused by a 2D to 3D structural change upon introduction of the impurity. After $n=8$, the drop in the polarizability from Na_{n+1} to Na_nLi is smaller (~3%), indicating that for large-size clusters, the effect of impurity is less prominent and they behave similar to the spherical jellium systems.

In Table I, we present the calculated polarizabilities along with the available experimental results and the earlier theoretical results [25]. The present calculations are in good agreement with the DFT/PW91 calculations. Our calculations reproduce the experimental trend for sodium-rich clusters with the error bar of approximately 10%. Our calculated polarizability for Li_3Na agrees within 4% with the experimental result. However, for Li_2Na, the calculated value overestimate experiment by as much as 45%. Since the calculated polarizability of the linear structure of Li_2Na is even higher than that of the triangular ground-state structure, this discrepancy cannot be attributed to the wrong identification of the ground state. In order to understand a possible cause of this discrepancy, we have run molecular-dynamics simulations for the Li_2Na cluster at $T=400$ K (temperature quoted in the experimental work) and calculated polarizabilities of several intermediate structures. We found that the polarizability of Li_2Na strongly depended on the cluster geometry and Li-Li and Li-Na bond lengths. For structures where the Li-Li bond length was reduced by approximately 15% and one of the Li-Na distances increased by 10%, the calculated polarizability was lower by almost 25% compared to the original ground-state structure. As such, it is possible that the discrepancy between theory and experiment for Li_2Na may be associated with the unstable structure of this cluster coupled with the effect of finite experimental temperature.

IV. CONCLUSIONS

In this paper, we have calculated the equilibrium geometries and polarizabilities of Na_nLi and Li_nNa ($n=1-12$) clusters. Our calculations were performed using *ab initio* molecular dynamics with the generalized gradient approximation for the exchange correlation potential. The resulting geometries of Na_nLi show that the Li atom becomes trapped in the Na cage for all clusters containing more than eight atoms. At the same time, our results for Li_nNa indicate that the Na atom prefers to be on the periphery and does not become trapped. We associate this effect with a larger ionic radius of Na compared to that of Li. Static polarizabilities of Na_nLi and Li_nNa were calculated using a finite-field technique. For both Na_nLi and Li_nNa clusters, the polarizabilities decrease with increasing the total number of atoms. Up to $n=8$ close shell system, the decrease is sharper, after which the decrease in polarizabilities slows down considerably and shows oscillatory behavior. Thus, it is seen that the effect of impurity on polarizability is significant on small clusters only. We find the polarizabilities of Li_nNa clusters to be lower than that for Na_nLi clusters, which could be explained by a stronger bonding in Li_nNa clusters as compared to Na_nLi.

ACKNOWLEDGMENTS

We gratefully acknowledge the Indo-French Center for the Promotion of Advanced Research (New Delhi) Centre Franco-Indian Pour la Promotion de la Recherche Avancee. I.V. and R.M.M. acknowledge support for this work by the National Science Foundation under Grant No. DMR 99-76550 for the Materials Computation Center at the University of Illinois and Grant No. DMR 98-02373. M.D. acknowledges the University Grants Commission, India, for financial support.

[1] U. Röthlisberger and W. Andreoni, J. Chem. Phys. **94**, 8129 (1991).
[2] R. O. Jones, A. I. Lichtenstein, and J. Hutter, J. Chem. Phys. **106**, 4566 (1997).
[3] R. O. Jones, J. Chem. Phys. **99**, 1194 (1993).
[4] V. Kumar and R. Car, Phys. Rev. B **44**, 8243 (1991).
[5] V. Bonačić-Koutecký, P. Fantucci, and J. Koutecký, Phys. Rev. B **37**, 4369 (1988); I. Boustani, W. Pewestorf, P. Fantucci, V. Bonačić-Koutecký, and J. Koutecký, *ibid.* **35**, 9437 (1987).
[6] G. Pacchioni, H. O. Beckmann, and Jaroslav Koutecký, J. Chem. Phys. **87**, 151 (1982).
[7] P. Fantucci, J. Koutecký, and G. Pacchioni, J. Chem. Phys. **80**, 325 (1984).
[8] B. K. Rao and P. Jena, Phys. Rev. B **32**, 2058 (1985).
[9] M. Deshpande, A. Dhavale, R. R. Zope, S. Chacko, and D. G. Kanhere, Phys. Rev. A **62**, 63202 (2000).
[10] Hai-Ping Cheng, R. N. Barnett, and Uzi Landman, Phys. Rev. B **48**, 1820 (1993).
[11] Yasuhiro Senda, Fuyuki Shimojo, and Kazo Hoshino, J. Phys. Soc. Jpn. **67**, 916 (1998).
[12] Ajeeta Dhavale, D. G. Kanhere, C. Majumdar, and G. P. Das, Eur. Phys. J. D **6**, 495 (1999).
[13] Rajendra R. Zope, S. A. Blundell, Tunna Baruah, and D. G. Kanhere, J. Chem. Phys. **115**, 2109 (2001).
[14] U. Röthlisberger and W. Andreoni, Int. J. Mod. Phys. B **6**, 3675 (1992).
[15] Ajeeta Dhavale, Vaishali Shah, and D. G. Kanhere, Phys. Rev. A **57**, 4522 (1998); R. R. Zope, S. A. Blundell, C. Guet, T.

Baruah, and D. G. Kanhere, *ibid.* **63**, 043202 (2001).
[16] C. Majumder, G. P. Das, S. K. Kulshrestha, V. Shah, and D. G. Kanhere, Chem. Phys. Lett. **261**, 515 (1996).
[17] Hidenori Matsuzawa, Toshiyuki Hanawa, Kazunori Suzuki, and Suehiro Iwata, Chem. Soc. Jpn. Bull. **65**, 2578 (1992).
[18] Ajeeta Dhavale, D. G. Kanhere, S. A. Blundell, and Rajendra R. Zope (unpublished).
[19] W. A. de Heer, Rev. Mod. Phys. **65**, 611 (1993).
[20] W. D. Knight, K. Clemenger, W. A. de Heer, and W. A. Saunders, Phys. Rev. B **31**, 2539 (1985).
[21] E. Benichou, R. Antoine, D. Rayane, B. Vezin, F. W. Dalby, Ph. Dugourd, M. Broyer, C. Ristori, F. Chandezon, B. A. Huber, J. C. Rocco, S. A. Blundell, and C. Guet, Phys. Rev. A **59**, R1 (1999).
[22] D. Rayane, A. R. Allouche, E. Benichou, R. Antine, M. Aubert-Frecon, Ph. Dugourd, M. Broyer, C. Ristori, F. Chandezon, B. A. Huber, and C. Guet, Eur. Phys. J. D **9**, 243 (1999).
[23] L. Kronik, I. Vasiliev, and J. R. Chelikowsky, Phys. Rev. B **62**, 9992 (2000); L. Kronik, I. Vasiliev, M. Jain, and J. R. Chelikowsky, J. Chem. Phys. **115**, 4322 (2001).
[24] S. Kümmel, T. Berkus, P. G. Reinhard, and M. Brack, Eur. Phys. J. D **11**, 239 (2000); I. Moullet, J. L. Martins, F. Reuse, and J. Buttet, Z. Phys. D: At., Mol. Clusters **12**, 353 (1989); M. Manninen, R. M. Nieminen, and M. J. Puska, Phys. Rev. B **33**, 4289 (1986); S. Kümmel, J. Akola, and M. Manninen, Phys. Rev. Lett. **84**, 3827 (2000).
[25] R. Antoine, D. Rayane, A. R. Allouche, M. Aubert-Frecon, E. Benichou, F. W. Dalby, Ph. Dugourd, and M. Broyer, J. Chem. Phys. **110**, 5568 (1999).
[26] D. C. Payne, J. D. Joannopoulos, D. C. Allan, M. P. Teter, D. H. Vanderbilt, Phys. Rev. Lett. **56**, 2656 (1986); M. C. Payne, M. P. Teter, D. C. Allan, T. A. Arias, and J. D. Joannopoulos, Rev. Mod. Phys. **64**, 1045 (1992).
[27] G. B. Bachelet, D. R. Hamann, and M. Schluter, Phys. Rev. B **26**, 4199 (1982).
[28] U. Barth and L. Hedin, J. Phys. C **5**, 1269 (1972).
[29] Igor Vasiliev, Serdar Ogut, and James R. Chelikowsky, Phys. Rev. Lett. **78**, 4805 (1997), and references therein.
[30] J. R. Chelikowsky, N. Troullier, and Y. Saad, Phys. Rev. Lett. **72**, 1240 (1994); J. R. Chelikowsky, N. Troullier, K. Wu, and Y. Saad, Phys. Rev. B **50**, 11 355 (1994).
[31] J. P. Perdew, J. A. Chevary, S. H. Vosko, K. A. Jackson, M. R. Pederson, D. J. Singh, and C. Fiolhais, Phys. Rev. B **46**, 6671 (1992); **48**, 4978 (1993).